ACS Catalysis

pubs.acs.org/acscatalysis

Research Article

A Redox-Switchable Gold(I) Complex for the Hydroamination of Acetylenes: A Convenient Way for Studying Ligand-Derived Electronic Effects

César Ruiz-Zambrana, Macarena Poyatos,* and Eduardo Peris*

Cite This: *ACS Catal.* 2022, 12, 4465−4472

Read Online

ACCESS | Metrics & More | Article Recommendations | Supporting Information

ABSTRACT: A gold complex with a naphthalene-di-imide-functionalized N-heterocyclic carbene (NHC) ligand was prepared and characterized. The electrochemical studies reveal that the complex is able to undergo two successive reduction events, associated to the reduction of the NDI moiety of the NHC ligand. Once the redox-switchable properties of this Au(I) complex were proven, the complex was tested in the hydroamination of terminal alkynes. The activity of the neutral complex was moderate-to-high for this reaction, but the one-electron reduced species did not show any activity in the reaction. The activity of the catalyst could be toggled off and on several times by successively adding a reducing agent (cobaltocene) or an oxidant (acetylferrocenium tetrafluoroborate). The results indicate that the rate-determining step of the catalytic cycle is the nucleophilic attack of the amine on the Au-coordinated alkyne.

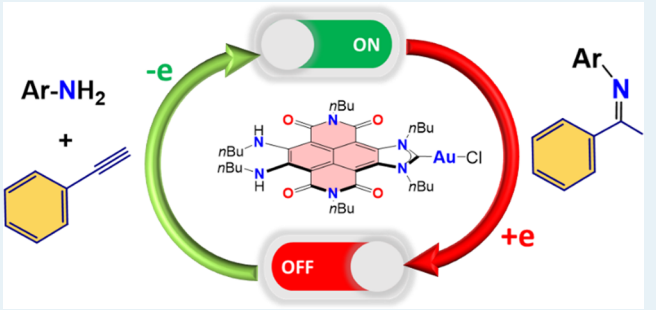

KEYWORDS: *redox-switchable, hydroamination of alkynes, gold, mechanism, N-heterocyclic carbene, homogeneous catalysis*

INTRODUCTION

During the past decade, gold complexes have flourished as the most attractive catalysts for the electrophilic activation of alkynes toward a large variety of nucleophiles.[1] The progress in the field has been boosted by the fact that new synthetic applications have been found and because detailed mechanistic studies have helped to unveil the essential features of these reactions. Gold complexes have been identified as efficient catalysts for the hydroamination of alkynes,[2] a process that can be regarded as the most atom-efficient method for the introduction of nitrogen fragments into organic molecules.[3] Detailed experimental and computational studies have been made in order to unveil the influence of the steric and electronic properties of phosphines[4] and N-heterocyclic carbene[5] (NHC) ligands on the hydroamination of alkynes. The first step of the catalytic cycle is the electrophilic activation of the alkyne, which is consequently favored by electron-poor ligands. The second step involves the nucleophilic attack of the amine on the alkyne, which is facilitated by electron-withdrawing ligands, providing a gold−vinyl intermediate. Then, the following step of the reaction is the so-called protonolysis (or protodeauration), which involves the migration of the proton from the N−H bond to the carbon bound to the gold atom and generates the final imine product. This step is accelerated by strong electron-donating ligands. Hence, the effect of the ligand electronic factors is ambivalent. The mechanistic studies suggest that the protonolysis is the rate-determining step (RDS) of the reaction, a conclusion that was also supported by some previous experimental studies.[6] However, exceptions to this general behavior have been observed. For example, the most strong electron-donating phosphines are not efficient in facilitating the hydroamination,[7] and the same trend was recently found for the case of mesoionic carbene (MIC) ligands,[8] although these observations may be ascribed to changes in the steric properties and/or stability of the catalyst concomitant to the changes in their electronic properties. In addition, the use of redox-switchable gold(I) catalysts shows that the activity of the in situ oxidized catalysts outperforms the activity of their reduced forms.[9] Redox-switchable ligands are useful to unveil mechanistic aspects of catalytic reactions because the electron-donating character of the ligand can be modulated without substantial changes in their steric properties. Therefore, these two last examples reveal that − at least for these particular cases − very likely, the RDS stage of the cycle is the nucleophilic addition of the amine to the triple bond of the alkyne, rather than the

Received: February 4, 2022
Revised: March 15, 2022
Published: March 31, 2022

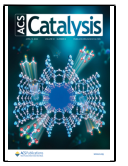

https://doi.org/10.1021/acscatal.2c00613
ACS Catal. 2022, 12, 4465−4472

Scheme 1. Preparation of NDI−NHC complexes 3−5

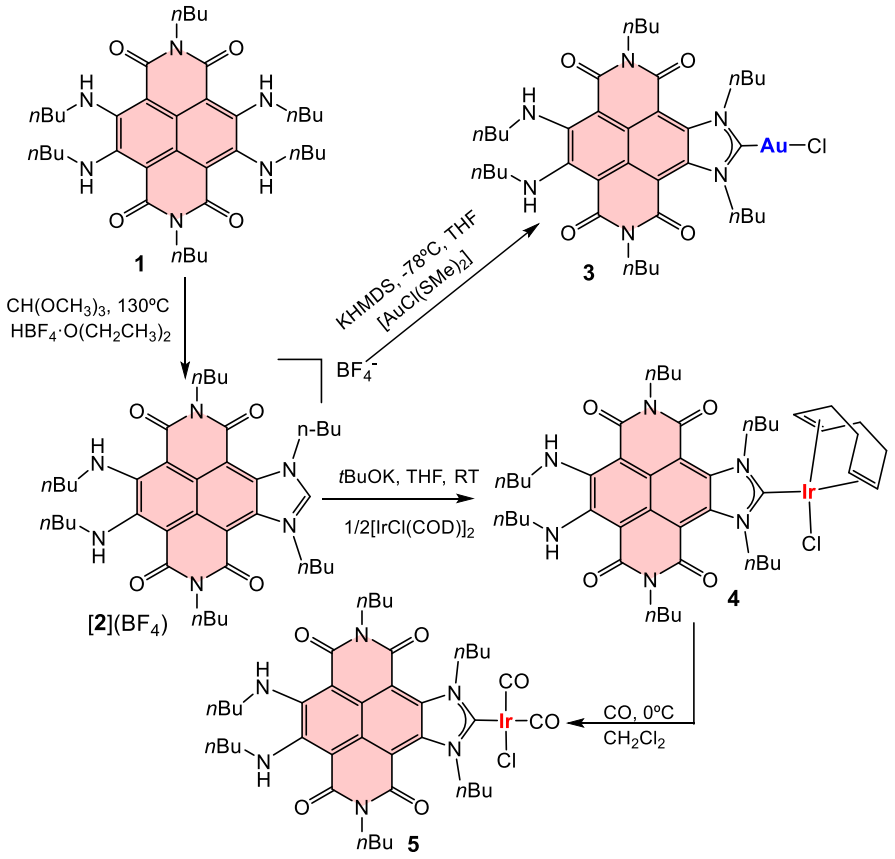

protodeauration. However, further strong evidence to support this conclusion is needed.

Redox-active ligands can modify their electron-donating character by accepting or releasing electrons.[10] This means that the catalytic activity (or selectivity) of the metal complex depends on whether the redox-active ligand is acting in its neutral or oxidized/reduced forms. NHC ligands have been particularly fruitful in the generation of photo-[11] and redox-switchable catalysts,[12] among which, gold−NHC complexes have provided a number of very interesting examples.[9b,13] Notably, ferrocene has been the cornerstone of gold-based redox-switchable catalysts[9,13,14] due to its amenability to synthetic modification, stability, and redox properties.

We recently described an NHC ligand functionalized with a naphthalene diimide (NDI) moiety that behaved as an effective redox-switchable ligand in the rhodium- and iridium-catalyzed cyclization of alkynoic acids.[15] Given that all redox-switchable gold catalysts tested in the hydroamination of alkynes used so far are based on ferrocenyl-containing complexes,[9a,14,16] we thought that the introduction of a NDI-functionalized ligand in this gold-catalyzed reaction could provide a new perspective that may shed some light on the mechanistic aspects of the process. Ferrocenyl-containing redox-switchable ligands allow us to change the redox state of the ligand between a neutral and an oxidized state; therefore, the redox event involves reducing the electron-donating character of the ligand upon oxidation. Our new NDI−NHC ligand can modulate its electronic character between three oxidation states, as the neutral ligand can enhance its electron-donating character upon two successive one-electron reductions. This means that the redox events shown by ferrocenyl- and NDI-functionalized ligands modify the electronic properties of the catalyst in exact opposite directions. Based on this idea, we now report the preparation of a new NDI−NHC ligand and its coordination to gold. The catalytic activity of this complex and its redox-switchable character were studied in the hydroamination of alkynes. As will be discussed in the following sections, these studies allow us to extract essential information regarding the mechanistic aspects of this catalytic reaction.

RESULTS AND DISCUSSION

The NDI-functionalized imidazolium salt [**2**](BF$_4$) was prepared by mono-annulation of NDI-tetraamine compound **1**,[17] with trimethylorthoformate in the presence of HBF$_4$, as depicted in Scheme 1. Note that [**2**](BF$_4$) is a mono-imidazolium salt resulting from the mono-cyclization of **1**; therefore, it differs from the NDI-functionalized bisazolium salt that we described recently.[15] The NDI-azolium salt [**2**](BF$_4$) was isolated as a reddish compound that was characterized by NMR spectroscopy and electrospray ionization mass spectrometry (ESI-MS). The ^{1}H NMR spectrum of [**2**](BF$_4$) shows the characteristic resonance due to the C2−H protic proton at 9.70 ppm. The ESI-MS spectrum shows the base peak at m/z = 673.736, assigned to [**2**$^+$]. The preparation of gold complex **3** was performed by deprotonating [**2**](BF$_4$) with potassium bis(trimethylsilyl)amide (KHMDS) at −78 °C, followed by addition of [AuCl(SMe)$_2$]. The ^{1}H NMR spectrum of **3** is consistent with the twofold symmetry of the molecule and shows that the signal due to the protic C2−H proton disappeared. The ^{13}C NMR spectrum shows the distinctive signal due to the Au−C$_{carbene}$ carbon at 186.6 ppm.

https://doi.org/10.1021/acscatal.2c00613
ACS Catal. 2022, 12, 4465−4472

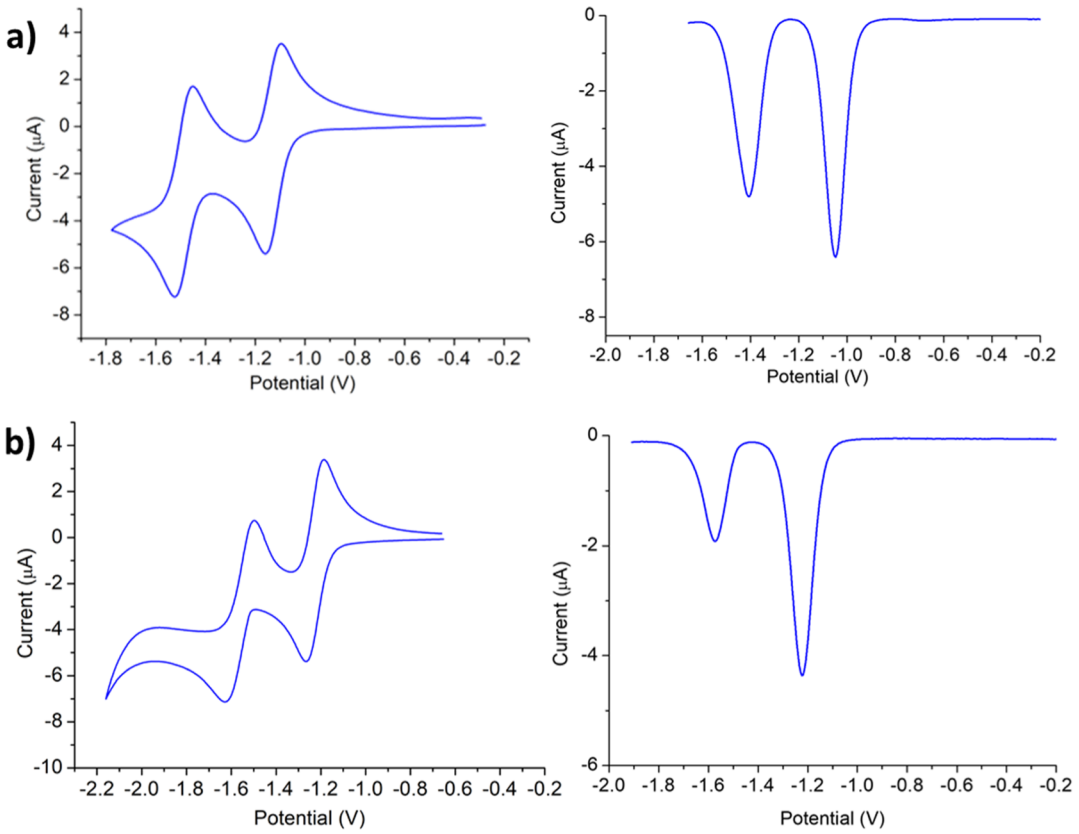

Figure 1. Cyclic Voltammograms and differential pulse voltammetry experiments (DPV) of [**2**](BF$_4$) (a) and **3** (b), in dry CH_2Cl_2 with a 0.1 mM analyte and 0.25 M [N(*n*Bu)$_4$][PF$_6$]. Measurements performed at 100 mV s^{-1} and referenced versus ferrocenium/ferrocene.

The cyclic voltammograms of [**2**](BF$_4$) and **3** are displayed in Figure 1. The CV data for [**2**](BF$_4$) reveal two reversible well-separated redox events associated with the sequential one-electron reductions of the NDI moiety of the imidazolium cation. The first process ($E_{1/2}$ = −1.05 V vs Fc$^+$/Fc) corresponds to the one-electron reduction of [**2**$^+$] to the radical neutral species [**2**$^\bullet$], while the second event ($E_{1/2}$ = −1.40 V vs Fc$^+$/Fc) is assigned to the formation of the doubly reduced anion [**2**$^-$]. For this data set, the peak potentials are independent of the scan rate, as expected for reversible processes (see the Supporting Information for full details). The cyclic voltammogram of **3** shows one reversible reduction wave ($E_{1/2}$ = −1.22 V vs Fc$^+$/Fc) followed by a second quasi-reversible process ($E_{1/2}$ = −1.55 V vs Fc$^+$/Fc). The peak potentials and peak separations of the first process are independent of the scan rate. For the second reduction event, E_p values are slightly shifted to more extreme potentials with increasing scan rates, thus indicating a quasi-reversible process.[18] In any case, these potentials are more negative than those shown for [**2**$^+$] as a consequence of the neutral character of **3** compared to the cationic nature of [**2**$^+$]. As the catalytic reactions that we will describe below were performed in the presence of NaBAR^F, we also performed electrochemical studies of **3** in the presence of NaBAR^F (see Figure S19 in the Supporting Information for details). These experiments showed that the first reduction wave was reversible and appeared at the same potential as that for **3** in the absence of NaBAR^F, while the second wave was irreversible. This experiment suggests that the non-reversible second reduction wave shown by **3** may be ascribed to the slow loss of the chloride ligand, as the addition of a chloride scavenger as NaBAR^F turns the second reduction event irreversible.

UV−vis spectroelectrochemical (SEC) studies were performed in order to retrieve information about the nature and stability of the species formed upon one- and two-electron reductions of [**2**](BF$_4$) and **3**. The experiments were performed using an optically transparent thin layer electrochemical (OTTLE) cell in CH_2Cl_2, by progressively applying more negative potentials while recording the corresponding UV−vis spectra. The resulting series of spectra can be seen in Figure 2. As can be observed in Figure 2a, the UV−vis spectrum of [**2**](BF$_4$) shows a vibronically resolved band with its maximum peak at 450 nm. Upon application of progressively increasing negative potentials, the band associated to [**2**$^+$] decreased, while a new vibronically coupled band at 550 nm attributed to the one-electron-reduced species [**2**$^\bullet$] appeared. Further electronic reduction gave rise to the appearance of two bands with peak maxima at 300 and 545 nm, assigned to the doubly reduced anion [**2**$^-$]. In a similar manner, UV−vis SEC experiments were performed using gold complex **3** (Figure 2b). The UV−vis spectrum of **3** shows one vibronically resolved band with its maximum peak at 545 nm, attributed to transitions centered in the NDI core of the NHC ligand. The application of progressively increasing negative potentials resulted in the decrease of this band, with the concomitant appearance of new featureless bands centered at 555, 425, and 310 nm associated with the formation of [**3**$^-$]. The application of more negative potentials resulted in the progressive disappearance of these three bands, with the concomitant appearance of a new weak band at 650 nm. These changes are due to the disappearance of [**3**$^-$] with the

https://doi.org/10.1021/acscatal.2c00613
ACS Catal. 2022, 12, 4465−4472

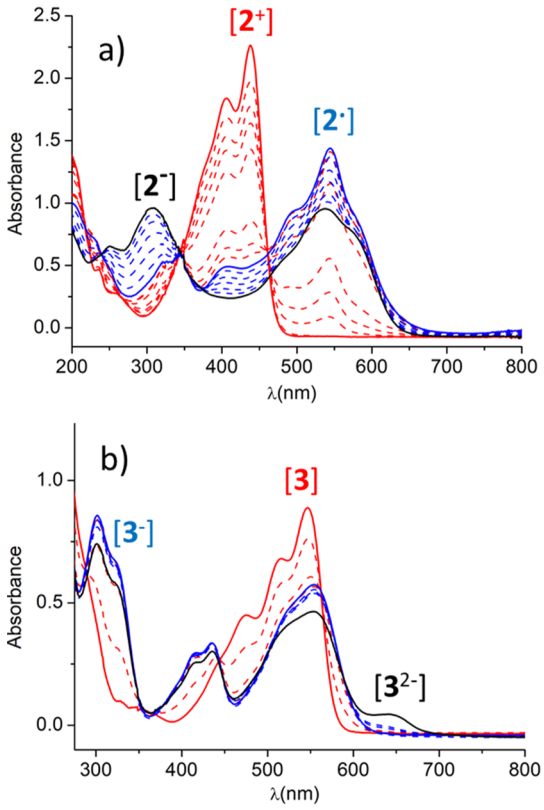

Figure 2. UV−vis SEC monitoring reduction of [**2**](BF$_4$) (a) and **3** (b) in CH_2Cl_2 {0.1 M [N(nBu)$_4$][PF$_6$]}. The electrochemical reduction was performed applying progressively lower potentials with a Au working electrode, Pt counter electrode, and Ag wire pseudo-reference electrode. The solid lines represent the spectra of the starting (red), singly reduced (blue), and doubly reduced (black) species.

concomitant appearance of the doubly reduced species [$\mathbf{3}^{2-}$], which is unstable. It is important to mention that the application of a positive potential once [$\mathbf{3}^{2-}$] was formed allowed us to recover only partially the starting neutral complex **3**. This is evidenced by the decrease in the intensity of resulting complex **3** obtained by a full cycle involving the **3** → [$\mathbf{3}^{-}$] → [$\mathbf{3}^{2-}$] → [$\mathbf{3}^{-}$] → **3** transformation, in agreement with the non-reversible (quasireversible) character of the [$\mathbf{3}^{-}$]→[$\mathbf{3}^{2-}$] step. On the contrary, when the process was allowed to produce the one-electron reduction alone [**3** → ($\mathbf{3}^{-}$)], application of a positive potential allowed us to fully recover original complex **3**, as a consequence of the reversibility of the first reduction step (see Figure 1b).

As we mentioned above, we expected that the reduction of the NDI-functionalized NHC should increase the electron-donating character of the ligand. In order to quantify this effect, we obtained iridium−carbonyl complex **5**, which was obtained by bubbling CO in a CH_2Cl_2 solution of [IrCl(NDI-NHC) (COD)] complex **4**, as it is shown in Scheme 1. The details about the preparation and characterization of **4** and **5** can be found in the Supporting Information. The IR (CH_2Cl_2) spectrum of **5** shows the two C−O stretching bands at 2068 and 1987 cm^{-1}, which translates to a Tolman electronic parameter (TEP) of 2053 cm^{-1} after using the well-accepted correlation.[19] This TEP value is very similar to that shown by our previously reported pyrene-functionalized NHC ligands.[20] To explore the relationship between the redox state of the NDI−NHC ligand and its donicity, we sought to perform infrared SEC experiments, which allowed us to measure the shift in the ν_{CO} of **5** upon reduction of the NDI unit. As can be observed in the series of spectra shown in Figure 3, the

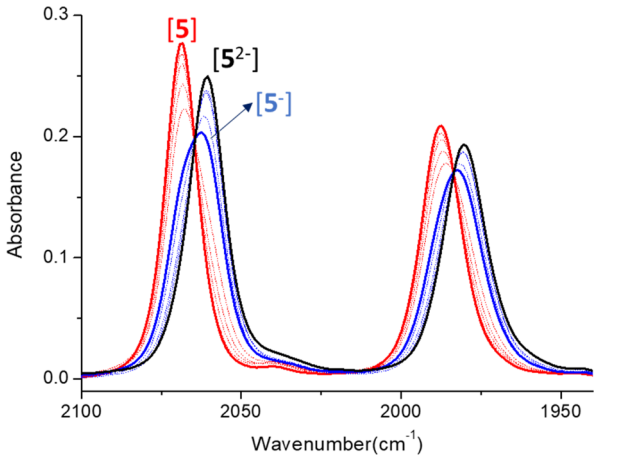

Figure 3. IR-SEC monitoring reduction of **5** in CH_2Cl_2 {0.1 M [N(nBu)$_4$][PF$_6$]}. The solid lines represent the IR spectra of **5** (red), [$\mathbf{5}^{\bullet-}$] (blue), and [$\mathbf{5}^{2-}$] (black) species.

progressive reduction of **5** is accompanied by a decrease in the intensity of the bands at 2068 and 1987 cm^{-1}, while two new bands appear at 2062 and 1982 cm^{-1}. These new bands are attributed to the one-electron reduced species [$\mathbf{5}^{\bullet-}$]. Further reduction to lower potentials results in the disappearance of the signals at 2062 and 1982 cm^{-1} and the appearance of a new set of bands at 2060 and 1980 cm^{-1}, which are assigned to the doubly reduced species [$\mathbf{5}^{2-}$]. This means that the first reduction produces an average Δ(CO) shift of −5.5 cm^{-1}, while the second reduction shifts ν(CO) by another −2 cm^{-1}, therefore indicating that the ligand is able to increase its electron-donating character in a two-step tunable way. We find important to point out that this Δ(CO) shift produced upon reduction of the NDI−NHC ligand is significantly lower compared to the shift that we observed for another related NDI-functionalized NHC ligand that we described recently.[15]

For the exploration of the catalytic activity of complex **3**, we decided to study the hydroamination of alkynes. As mentioned in the introduction, several studies have shown that the RDS of this reaction is the protodeauration.[4,5] However, some authors,[9a,21] including us,[9b] have reported that the presence of ligands on the Au(I) coordination sphere that is amenable to oxidation shows how the oxidized form of the complex outperforms the activity of the neutral form. Given that the oxidation of the redox-active ligand features a more acidic gold center and thus increases the electrophilicity of the coordinated alkyne ligand, these latter results point toward the nucleophilic attack on the alkyne as the RDS of the catalytic cycle, as was already pointed out recently by Paradies, Breher, and co-workers.[9a] In this scenario, we thought that the presence of a ligand that is amenable to reduction in complex **3** could provide a good insight for clarifying this controversy.

We first tested the activity of **3** in the hydroamination of phenylacetylene with four different amines. The reactions were performed in acetonitrile at 90 °C, using NaBAR^F as the chloride scavenger, and the evolution of the reaction was monitored by gas chromatography (GC). As can be observed from the data shown in Table 1, using a catalyst loading of 1

https://doi.org/10.1021/acscatal.2c00613
ACS Catal. 2022, 12, 4465−4472

Table 1. Activity of Complex 3 in the Hydroamination of Phenylacetylene with Arylamines[a]

entry	aryl	cat. load. (%)	additive	time (h)	yield (%)[b]
1	Ph	1	none	8	82.5
2	2-MeC_6H_4	1	none	8	77.2
3	4-MeC_6H_4	1	none	8	75.3
4	2,4,6-$Me_3C_6H_2$	1	none	8	76.9
5	Ph	0.5	none	8	49.2
6	Ph	2	none	5	90.0
7[c]	Ph	1	[$CoCp_2$]	8	0

[a]Reaction conditions: 0.5 mmol phenylacetylene, 0.55 mmol aryl amine, 1 mol % **3**, and 2 mol % $NaBAR^F$ in 1 mL of CH_3CN at 90 °C. [b]Yields calculated by GC using anisole (0.5 mmol) as the internal standard. Final yields were also confirmed by ^1H NMR spectroscopy. [c]One equivalent of cobaltocene was added related to the amount of the catalyst.

mol % produced yields of the imine products in the range of 75−82% after 8 h of reaction. For the case of the reaction between phenylacetylene and aniline, reduction of the catalyst loading to 0.5 mol % produces a significant decrease in the yield down to 49% (entry 5), while doubling the amount to 2 mol % increases the product yield up to 90% in just 5 h (entry 6).

Next, we performed kinetic studies in order to determine the reaction rate orders with respect to the catalyst and to the two substrates of the reaction. For the determination of the reaction order in the catalyst, we used the variable time normalization analysis, which consists of the visual comparison of the variably normalized concentration profiles.[22] The catalytic reactions were monitored using three different concentrations of **3** (0.5, 1, and 2 mol %). As can be observed from the graphic shown in Figure 4a, the normalized profiles match with a first order in **3** (the Supporting Information shows the normalized concentration profiles for a 0, 0.5, and 2 order in the catalyst). The reaction order in phenylacetylene and aniline was determined by measuring the initial rates of the reaction by changing the concentration of one of the substrates while maintaining a constant concentration of the other one. As can be seen from the linear fitting of the plots shown in Figure 4b,c, the reactions showed a first-order dependence on both substrates, which suggests that both of them are involved in the rate-limiting step, in agreement with previous reports.[5a] These data are also in agreement with a mechanism that falls into the category of reactions involving the nucleophilic attack of an amine on a gold-activated alkyne, followed by the nucleophile-assisted nitrogen-to-carbon atom−proton transfer.[5b,23]

In order to determine the effect of the increase in the electron-donating ability of the ligand in this catalytic reaction, we performed the studies in the presence of cobaltocene. With a redox potential of −1.33 V (vs Fc^+/Fc),[24] cobaltocene is a suitable additive for the one-electron reduction of our Au−NHC catalyst since the first reduction potential of **3** is −1.12 V. When the reaction between phenylacetylene and aniline was performed using a 1 mol % loading of **3** and the same amount of cobaltocene, we observed that the reaction produced negligible amounts of the imine product (Table 1, entry 7). This result could be ascribed to the deactivation of the catalyst as a consequence of the increasing electron-donating character of the ligand in [3^-] with respect to the neutral catalyst **3**. This

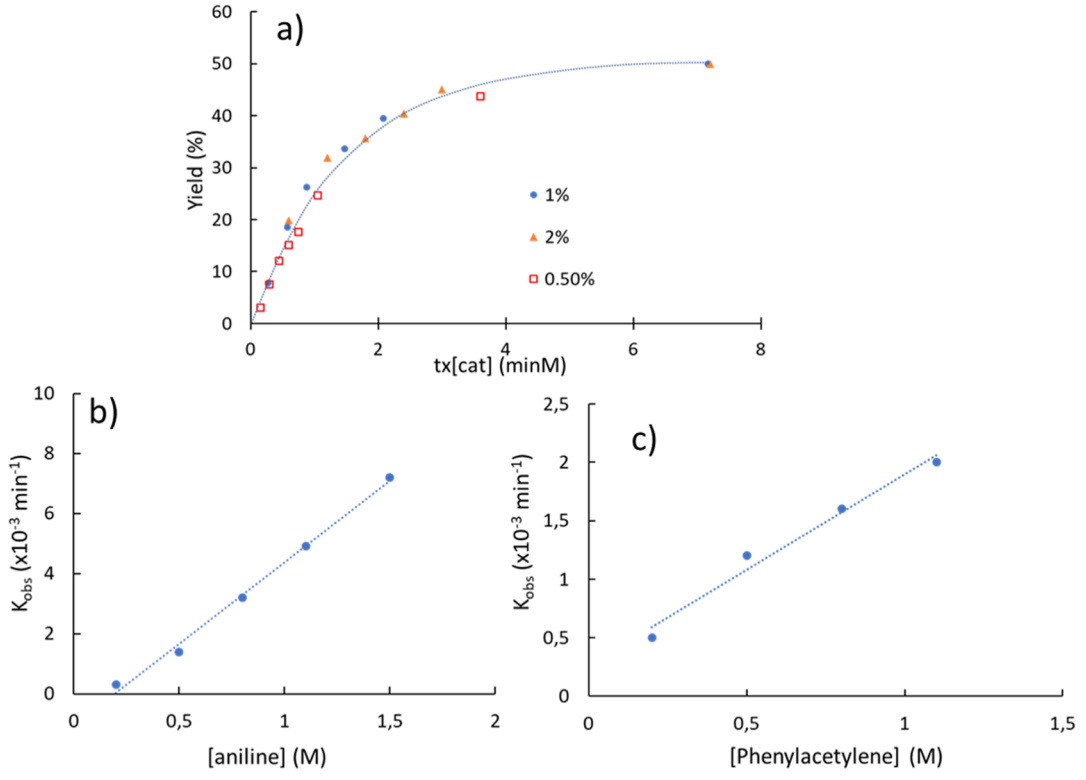

Figure 4. Determination of the reaction order with respect to the catalyst (a), aniline (b), and phenylacetylene (c). The determination of the order with respect to the catalyst was determined by using the variable time normalization analysis,[22b] while the order on the substrates was determined using the method of initial rates.

https://doi.org/10.1021/acscatal.2c00613
ACS Catal. 2022, 12, 4465−4472

interpretation would be in favor of considering the nucleophilic attack on the triple bond of the alkyne as the RDS of the catalytic process. However, the suppression of the activity of the reduced catalyst could also be attributed to the decomposition of the catalyst during the reaction, a possibility that we could not discard even though the CV studies and the SEC experiments showed that [**3**$^-$] is a rather stable species. In order to obtain stronger evidence about the influence of the electron-donating process in the reaction, we decided to evaluate if we could toggle between the active and inactive forms of the catalyst along the course of the reaction (Figure 5). First, we allowed the reaction to evolve for 90 min at 90 °C

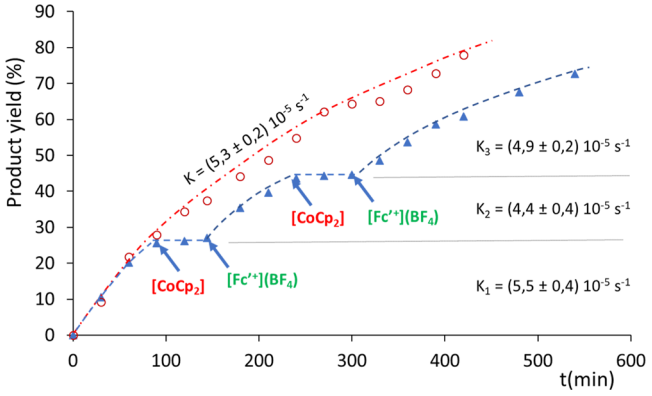

Figure 5. Plots showing the hydroamination of phenylacetylene with aniline using 1 mol % of **3** (red empty circles) and with sequential additions of cobaltocene and [Fe(η^5-$C_5H_4COCH_3$)Cp](BF$_4$) [(Fc'$^+$)(BF$_4$)] (blue triangles). The reactions were performed in CH_3CN at 90 °C, using phenylacetylene (0.5 mM) and aniline (0.55 mM). The evolution of the reaction was monitored by GC, using anisole as the internal standard. Final yields were also corroborated by ^{1}H NMR spectroscopy. The rate constants were obtained assuming a first-order reaction (see the Supporting Information).

in the presence of **3** (1 mol %), and we observed that the reaction evolved until 25% of product formation. Then, one equivalent of [$CoCp_2$] was added; thus, the catalyst was transformed to [**3**$^-$], which showed null activity during the following 60 min. After this time, acetylferrocenium tetrafluoroborate {[Fe(η^5-$C_5H_4COCH_3$)Cp](BF$_4$)} was added in order to oxidize the catalyst back to its active form, **3**, and we let the reaction to evolve for 90 min, after which 44% of the product was formed. The experiment was repeated by subsequent additions of [$CoCp_2$] and [Fe(η^5-$C_5H_4COCH_3$)Cp](BF$_4$), which allowed us to produce a total of two activation and deactivation cycles. An interesting point is that the activity of the catalyst can be restored almost completely after each addition of [Fe(η^5-$C_5H_4COCH_3$)Cp](BF$_4$), as can be observed by comparing the three rate constants obtained for the time gaps when the catalyst was in its active form (Figure 5). To make the comparison clearer, Figure 5 also represents the results of a parallel experiment showing the time-dependent reaction profile of the hydroamination of phenylacetylene with aniline using 1 mol % of **3**, without the addition of any external redox additive. A quick visual analysis of this plot allows us to observe that this profile is perfectly parallel to the profile in which the catalyst is active in the switch-on/switch-off experiment, all along the reaction profile. This experiment shows that the catalyst can be "switched off" upon addition of [$CoCp_2$] but also and more importantly that it can be further "switched on" upon addition of an oxidant, thus strongly suggesting that the addition of cobaltocene does not decompose the catalyst but transforms it into a dormant form. This observation clearly demonstrates that the catalyst is stable in both the active (neutral)/inactive (reduced) states and that the extended durations in the inactive form do still allow full recovery of the activity upon subsequent oxidation.

CONCLUSIONS

In summary, we prepared a naphthalene-di-imide-functionalized NHC ligand that was coordinated to gold(I). The CV studies reveal that the complex exhibits two reduction events, with the first one being reversible. The SEC analysis of the complex shows that the first reduction produces a species that is sufficiently stable to reversibly return to the original neutral species without observable decay of the intensity of the bands of the Uv−Vis spectrum. The NDI−NHC−Au(I) complex was tested in the hydroamination of phenylacetylene with four different anilines, where it showed good activity in the production of the resulting imine. On the other hand, the reactions carried out in the presence of cobaltocene resulted in the complete deactivation of the catalyst. In addition, the neutral catalyst can be deactivated and further activated several times without detectable decay of activity of the neutral (activated) form. These results give clear evidence that the activity of the catalyst is quenched when the ligand is reduced with the concomitant increase in its electron-donating strength, therefore strongly suggesting that the RDS of the catalytic cycle is the nucleophilic attack of the amine on the triple bond of the gold-coordinated alkyne. This conclusion becomes even more evident when we combine our results with those published previously regarding the use of other redox-switchable gold(I) catalysts with ligands that are amenable to oxidation,[9] for which the oxidation of the ligand results in the enhancement of the activity of the catalyst.

Our results also highlight the importance of redox-switchable catalysts for elucidating mechanistic aspects of a catalytic cycle. We think that the study of the influence of the electron-donating of the ligand in a catalytic process can be performed more accurately by using ligands with tunable electron-donating power, than by systematically changing the nature of the ligands. The studies performed by changing ligands are accompanied by a modification of a number of factors (electron-donating power, steric crowding, stability, etc.) that may lead to misinterpretations of the results, while the studies performed with redox-active ligands may provide accurate information about the electronic nature of the ligand while maintaining all other parameters untouched.

ASSOCIATED CONTENT

Supporting Information

The Supporting Information is available free of charge at https://pubs.acs.org/doi/10.1021/acscatal.2c00613.

Experimental details about the synthesis, characterization and catalytic experiments, and electrochemical and spectroelectrochemical studies (PDF)

AUTHOR INFORMATION

Corresponding Authors

Macarena Poyatos − *Institute of Advanced Materials (INAM), Centro de Innovación en Química Avanzada (ORFEO-CINQA), Universitat Jaume I^{RINGGOLD}, Castellón*

https://doi.org/10.1021/acscatal.2c00613
ACS Catal. 2022, 12, 4465−4472

E-12071, Spain; orcid.org/0000-0003-2000-5231; Email: poyatosd@uji.es

Eduardo Peris − *Institute of Advanced Materials (INAM), Centro de Innovación en Química Avanzada (ORFEO-CINQA), Universitat Jaume I[RINGGOLD], Castellón E-12071, Spain;* orcid.org/0000-0001-9022-2392; Email: eperis@uji.es

Author

César Ruiz-Zambrana − *Institute of Advanced Materials (INAM), Centro de Innovación en Química Avanzada (ORFEO-CINQA), Universitat Jaume I[RINGGOLD], Castellón E-12071, Spain;* orcid.org/0000-0003-4208-0929

Complete contact information is available at: https://pubs.acs.org/10.1021/acscatal.2c00613

Author Contributions

The article was written through contributions of all authors. All authors have given approval to the final version of the article.

Funding

Financial support from the Ministerio de Ciencia y Universidades (PGC2018-093382-B-I00) and the Universitat Jaume I (UJI-B2020-01 and UJI-B2018-46).

Notes

The authors declare no competing financial interest.

■ ACKNOWLEDGMENTS

We gratefully acknowledge financial support from the Ministerio de Ciencia y Universidades (PGC2018-093382-B-I00) and the Universitat Jaume I (UJI-B2020-01 and UJI-B2018-46). We are grateful to the Serveis Centrals d'Instrumentació Científica (SCIC-UJI) for providing us with spectroscopic facilities. We also want to thank Dr. A. Gutiérrez-Blanco (UJI) for helping in the preparation of the NDI-functionalized azolium salt and complex **3**.

■ ABBREVIATIONS

NDI naphthalene-di-imide
NHC N-heterocyclic carbene
SEC spectroelectrochemical

■ REFERENCES

(1) (a) Arcadi, A. Alternative synthetic methods through new developments in catalysis by gold. *Chem. Rev.* **2008**, *108*, 3266−3325. (b) Benitez, D.; Shapiro, N. D.; Tkatchouk, E.; Wang, Y.; Goddard, W. A., III; Toste, F. D. A bonding model for gold(I) carbene complexes. *Nat. Chem.* **2009**, *1*, 482−486. (c) Praveen, C. Carbophilic activation of pi-systems via gold coordination: Towards regioselective access of intermolecular addition products. *Coord. Chem. Rev.* **2019**, *392*, 1−34. (d) Jiménez-Núñez, E.; Echavarren, A. M. Gold-catalyzed cycloisomerizations of enynes: A mechanistic perspective. *Chem. Rev.* **2008**, *108*, 3326−3350. (e) Li, Z.; Brouwer, C.; He, C. Gold-catalyzed organic transformations. *Chem. Rev.* **2008**, *108*, 3239−3265. (f) Shapiro, N. D.; Toste, F. D. A Reactivity-Driven Approach to the Discovery and Development of Gold-Catalyzed Organic Reactions. *Synlett* **2010**, *2010*, 675−691. (g) Zeng, X. Recent Advances in Catalytic Sequential Reactions Involving Hydroelement Addition to Carbon-Carbon Multiple Bonds. *Chem. Rev.* **2013**, *113*, 6864−6900. (h) Tang, X.-T.; Yang, F.; Zhang, T.-T.; Liu, Y.-F.; Liu, S.-Y.; Su, T.-F.; Lv, D.-C.; Shen, W.-B. Recent Progress in N-Heterocyclic Carbene Gold-Catalyzed Reactions of Alkynes Involving Oxidation/Amination/Cycloaddition. *Catalysts* **2020**, *10*, 350. (i) Dorel, R.; Echavarren, A. M. Gold(I)-Catalyzed Activation of Alkynes for the Construction of Molecular Complexity. *Chem. Rev.* **2015**, *115*, 9028−9072. (j) Hashmi, A. S. K. Gold-catalyzed organic reactions. *Chem. Rev.* **2007**, *107*, 3180−3211.

(2) (a) Mizushima, E.; Hayashi, T.; Tanaka, M. Au(I)-catalyzed highly efficient intermolecular hydroamination of alkynes. *Org. Lett.* **2003**, *5*, 3349−3352. (b) Patil, N. T.; Kavthe, R. D.; Raut, V. S.; Shinde, V. S.; Sridhar, B. Gold- and Platinum-Catalyzed Formal Markownikoff's Double Hydroamination of Alkynes: A Rapid Access to Tetrahydroquinazolinones and Angularly-Fused Analogues Thereof. *J. Org. Chem.* **2010**, *75*, 1277−1280. (c) Zhang, J.; Yang, C.-G.; He, C. Gold(I)-catalyzed intra- and intermolecular hydroamination of unactivated olefins. *J. Am. Chem. Soc.* **2006**, *128*, 1798−1799. (d) Widenhoefer, R. A.; Han, X. Gold-catalyzed hydroamination of C-C multiple bonds. *Eur. J. Org. Chem.* **2006**, *2006*, 4555−4563. (e) Leung, C. H.; Baron, M.; Biffis, A. Gold-Catalyzed Intermolecular Alkyne Hydrofunctionalizations-Mechanistic Insights. *Catalysts* **2020**, *10*, 1210. (f) Lavallo, V.; Frey, G. D.; Donnadieu, B.; Soleilhavoup, M.; Bertrand, G. Homogeneous catalytic hydroamination of alkynes and allenes with ammonia. *Angew. Chem., Int. Ed.* **2008**, *47*, 5224−5228. (g) Akana, J. A.; Bhattacharyya, K. X.; Müller, P.; Sadighi, J. P. Reversible C-F bond formation and the Au-catalyzed hydrofluorination of alkynes. *J. Am. Chem. Soc.* **2007**, *129*, 7736−7737.

(3) Müller, T. E.; Hultzsch, K. C.; Yus, M.; Foubelo, F.; Tada, M. Hydroamination: Direct addition of amines to alkenes and alkynes. *Chem. Rev.* **2008**, *108*, 3795−3892.

(4) Wang, W.; Hammond, G. B.; Xu, B. Ligand Effects and Ligand Design in Homogeneous Gold(I) Catalysis. *J. Am. Chem. Soc.* **2012**, *134*, 5697−5705.

(5) (a) Yazdani, S.; Junor, G. P.; Peltier, J. L.; Gembicky, M.; Jazzar, R.; Grotjahn, D. B.; Bertrand, G. Influence of Carbene and Phosphine Ligands on the Catalytic Activity of Gold Complexes in the Hydroamination and Hydrohydrazination of Alkynes. *ACS Catal.* **2020**, *10*, 5190−5201. (b) Couce-Rios, A.; Kovács, G.; Ujaque, G.; Lledós, A. Hydroamination of C-C Multiple Bonds with Hydrazine Catalyzed by N-Heterocyclic Carbene-Gold(I) Complexes: Substrate and Ligand Effects. *ACS Catal.* **2015**, *5*, 815−829. (c) Kovács, G.; Lledos, A.; Ujaque, G. Hydroamination of Alkynes with Ammonia: Unforeseen Role of the Gold(I) Catalyst. *Angew. Chem., Int. Ed.* **2011**, *50*, 11147−11151.

(6) (a) Hashmi, A. S. K.; Schuster, A. M.; Rominger, F. Gold Catalysis: Isolation of Vinylgold Complexes Derived from Alkynes. *Angew. Chem., Int. Ed.* **2009**, *48*, 8247−8249. (b) Hashmi, A. S. K.; Ramamurthi, T. D.; Rominger, F. On the Trapping of Vinylgold Intermediates. *Adv. Synth. Catal.* **2010**, *352*, 971−975. (c) Gaggioli, C. A.; Ciancaleoni, G.; Zuccaccia, D.; Bistoni, G.; Belpassi, L.; Tarantelli, F.; Belanzoni, P. Strong Electron-Donating Ligands Accelerate the Protodeauration Step in Gold(I)-Catalyzed Reactions: A Quantitative Understanding of the Ligand Effect. *Organometallics* **2016**, *35*, 2275−2285.

(7) Witteler, T.; Darmandeh, H.; Mehlmann, P.; Dielmann, F. Dialkyl(1,3-diarylimidazolin-2-ylidenamino)phosphines: Strongly Electron-Donating, Buchwald-Type Phosphines. *Organometallics* **2018**, *37*, 3064−3072.

(8) Beerhues, J.; Walter, R. R. M.; Aberhan, H.; Neubrand, M.; Porré, M.; Sarkar, B. Spotlight on Ligand Effects in 1,2,3-Triazolylidene Gold Complexes for Hydroamination Catalysis: Synthesis and Catalytic Application of an Activated MIC Gold Triflimide Complex and Various MIC Gold Chloride Complexes. *Organometallics* **2021**, *40*, 1077−1085.

(9) (a) Deck, E.; Wagner, H. E.; Paradies, J.; Breher, F. Redox-responsive phosphonite gold complexes in hydroamination catalysis. *Chem. Commun.* **2019**, *55*, 5323−5326. (b) Ibáñez, S.; Poyatos, M.; Dawe, L. N.; Gusev, D.; Peris, E. Ferrocenyl-Imidazolylidene Ligand for Redox-Switchable Gold-Based Catalysis. A Detailed Study on the Redox-Switching Abilities of the Ligand. *Organometallics* **2016**, *35*, 2747−2758.

(10) (a) Allgeier, A. M.; Mirkin, C. A. Ligand design for electrochemically controlling stoichiometric and catalytic reactivity of transition metals. *Angew. Chem., Int. Ed.* **1998**, *37*, 894−908. (b) Berben, L. A.; de Bruin, B.; Heyduk, A. F. Non-innocent ligands.

Chem. Commun. **2015**, *51*, 1553−1554. (c) Lyaskovskyy, V.; de Bruin, B. Redox Non-Innocent Ligands: Versatile New Tools to Control Catalytic Reactions. *ACS Catal.* **2012**, *2*, 270−279. (d) Hindson, K.; de Bruin, B. Special Issue: Cooperative & Redox Non-Innocent Ligands in Directing Organometallic Reactivity (Cluster Issue). *Eur. J. Inorg. Chem.* **2012**, 340−342. (e) Luca, O. R.; Huang, D. L.; Takase, M. K.; Crabtree, R. H. Redox-active cyclopentadienyl Ni complexes with quinoid N-heterocyclic carbene ligands for the electrocatalytic hydrogen release from chemical fuels. *New J. Chem.* **2013**, *37*, 3402−3405.

(11) (a) Shao, H.; Wang, Y.; Bielawski, C. W.; Liu, P. Computational Investigations of the Effects of N-Heterocyclic Carbene Ligands on the Mechanism, Reactivity, and Regioselectivity of Rh-Catalyzed Hydroborations. *ACS Catal.* **2020**, *10*, 3820−3827. (b) Neilson, B. M.; Bielawski, C. W. Photoswitchable Metal-Mediated Catalysis: Remotely Tuned Alkene and Alkyne Hydroborations. *Organometallics* **2013**, *32*, 3121−3128.

(12) Ryu, Y.; Ahumada, G.; Bielawski, C. W. Redox- and light-switchable N-heterocyclic carbenes: a "soup-to-nuts" course on contemporary structure-activity relationships. *Chem. Commun.* **2019**, *55*, 4451−4466.

(13) (a) Klenk, S.; Rupf, S.; Suntrup, L.; van der Meer, M.; Sarkar, B. The Power of Ferrocene, Mesoionic Carbenes, and Gold: Redox-Switchable Catalysis. *Organometallics* **2017**, *36*, 2026−2035. (b) Hettmanczyk, L.; Suntrup, L.; Klenk, S.; Hoyer, C.; Sarkar, B. Heteromultimetallic Complexes with Redox-Active Mesoionic Carbenes: Control of Donor Properties and Redox-Induced Catalysis. *Chem.—Eur. J.* **2017**, *23*, 576−585. (c) Hettmanczyk, L.; Manck, S.; Hoyer, C.; Hohloch, S.; Sarkar, B. Heterobimetallic complexes with redox-active mesoionic carbenes as metalloligands: electrochemical properties, electronic structures and catalysis. *Chem. Commun.* **2015**, *51*, 10949−10952.

(14) Straube, A.; Coburger, P.; Dütsch, L.; Hey-Hawkins, E. Triple the fun: tris(ferrocenyl)arene-based gold(i) complexes for redox-switchable catalysis. *Chem. Sci.* **2020**, *11*, 10657−10668.

(15) Ruiz-Zambrana, C.; Gutierrez-Blanco, A.; Gonell, S.; Poyatos, M.; Peris, E. Redox-Switchable Cycloisomerization of Alkynoic Acids with Napthalenediimide-Derived N-Heterocyclic Carbene Complexes. *Angew. Chem., Int. Ed.* **2021**, *60*, 20003−20011.

(16) Ibáñez, S.; Poyatos, M.; Peris, E. Gold Catalysts with Polyaromatic-NHC ligands. Enhancement of Activity by Addition of Pyrene. *Organometallics* **2017**, *36*, 1447−1451.

(17) Sasikumar, M.; Suseela, Y. V.; Govindaraju, T. Dibromohydantoin: A Convenient Brominating Reagent for 1,4,5,8-Naphthalenetetracarboxylic Dianhydride. *Asian J. Org. Chem.* **2013**, *2*, 779−785.

(18) Wang, H.; Sayed, S. Y.; Luber, E. J.; Olsen, B. C.; Shirurkar, S. M.; Venkatakrishnan, S.; Tefashe, U. M.; Farquhar, A. K.; Smotkin, E. S.; McCreery, R. L.; Buriak, J. M. Redox Flow Batteries: How to Determine Electrochemical Kinetic Parameters. *ACS Nano* **2020**, *14*, 2575−2584.

(19) Kelly, R. A., III; Clavier, H.; Giudice, S.; Scott, N. M.; Stevens, E. D.; Bordner, J.; Samardjiev, I.; Hoff, C. D.; Cavallo, L.; Nolan, S. P. Determination of N-heterocyclic carbene (NHC) steric and electronic parameters using the (NHC)Ir(CO)2Cl system. *Organometallics* **2008**, *27*, 202−210.

(20) (a) Gonell, S.; Poyatos, M.; Peris, E. Pyrene-Based Bisazolium Salts: From Luminescence Properties to Janus-Type Bis-N-Heterocyclic Carbenes. *Chem.—Eur. J.* **2014**, *20*, 9716−9724. (b) Valdés, H.; Poyatos, M.; Peris, E. A Pyrene-Based N-Heterocyclic Carbene: Study of Its Coordination Chemistry and Stereoelectronic Properties. *Organometallics* **2014**, *33*, 394−401.

(21) Yang, H.; Gabbaï, F. P. Activation of a Hydroamination Gold Catalyst by Oxidation of a Redox-Noninnocent Chlorostibine Z-Ligand. *J. Am. Chem. Soc.* **2015**, *137*, 13425−13432.

(22) (a) Burés, J. A Simple Graphical Method to Determine the Order in Catalyst. *Angew. Chem., Int. Ed.* **2016**, *55*, 2028−2031. (b) Burés, J. Variable Time Normalization Analysis: General Graphical Elucidation of Reaction Orders from Concentration Profiles. *Angew. Chem., Int. Ed.* **2016**, *55*, 16084−16087.

(23) Lu, Z.; Hammond, G. B.; Xu, B. Improving Homogeneous Cationic Gold Catalysis through a Mechanism-Based Approach. *Acc. Chem. Res.* **2019**, *52*, 1275−1288.

(24) Connelly, N. G.; Geiger, W. E. Chemical redox agents for organometallic chemistry. *Chem. Rev.* **1996**, *96*, 877−910.

https://doi.org/10.1021/acscatal.2c00613
ACS Catal. 2022, 12, 4465−4472